doi: 10.18323/2782-4039-2023-3-65-1

The profile physical coefficient and its application for modelling the machined surface texture

Igor N. Bobrovskij, Doctor of Sciences (Engineering), researcher
Togliatti State University, Togliatti (Russia)

E-mail: bobri@yandex.ru ORCID: https://orcid.org/0000-0002-9513-7936

Received 28.07.2022 *Accepted 14.04.2023*

Abstract: Current trends in the development of mechanical engineering impose increasingly stringent requirements for the performance characteristics of manufactured goods. The main parameters characterizing the quality of a product as a whole are the physical, mechanical, and geometric indicators of the working surfaces of the compound units. In domestic practice, a machined surface is mainly characterized by a rather limited number of parameters (no more than 6), such as the average microroughness height, the microroughness height at 10 points, etc. However, their use is not enough to manufacture competitive products in the modern conditions. For example, international ISO/ASME/DIN standards include a much broader set of parameters required to accurately describe the performance properties of a surface. The paper analyzes the approaches to the formation of requirements for the microgeometry of the working surfaces of parts used in modern mechanical engineering. Based on the analysis, the author proposed and mathematically substantiated a general approach to modelling surface texture characteristics, which allows describing adequately the surface using a new parameter – the profile physical coefficient, since it is virtually impossible to directly compare the technologies developed in Russia with foreign analogues based on the current standards. First, the profile physical coefficient was determined at the section level. Next, it was decomposed into a Fourier series for the two-dimensional and three-dimensional cases. The paper presents the analysis of the new parameter applicability on the example of a product obtained by honing. The author concluded about the applicability of this parameter and the necessity to develop a comprehensive methodology based on it for evaluating the surface after machining.

Keywords: mechanical engineering technology; machining; surface; profile physical coefficient; rough layer; surface texture.

Acknowledgements: The research was supported by a grant from the Russian Science Foundation (Project No. 20-79-00233, https://rscf.ru/project/20-79-00233/).

For citation: Bobrovskij I.N. The profile physical coefficient and its application for modelling the machined surface texture. *Frontier Materials & Technologies*, 2023, no. 3, pp. 9–17. DOI: 10.18323/2782-4039-2023-3-65-1.

INTRODUCTION

The characteristics and surface texture of products are regulated by the international standards, such as ISO/TR 14638, as well as by the chain of standards for surface texture. By now, the roughness profile and the parameters defining it represent but a few characteristics of the surface texture, which are clearly normalised. Surface texture parameters – a primary profile, waviness, and roughness are defined by the ISO 4287:1997 International Standard, as well as by the ISO 3274:1996 Geometrical Product Specification (GPS). Surface structure. Profile method. Rated characteristics of contact (stylus) instruments. The terminology used in mathematical modelling corresponds to the list of accepted international standards:

– ISO 4288:1996 Geometrical Product Characteristics (GPP). Surface structure. Profile method. Rules and procedures for assessing surface structure;

– ISO 11562:1996 Geometrical Product Specification (GPS). Surface structure. Profile method. Metrological characteristics of filters with phase correction;

– ASME B46.1-2009. Surface Texture (Surface Roughness, Waviness, and Lay).

Basic terms:

– profile filter – according to ISO 21920-2 and ISO 16610-21, divides the profile into long-wave and short-wave components;

– real surface – limits the body, separating it from the environment;

– surface profile – is formed as a result of the intersection of a real surface with a special plane parallel to the *XOZ* and *YOZ* coordinate planes;

– primary profile – is regulated by ISO 3274 and serves as the basis for obtaining quantitative evaluation characteristics;

– surface profile – is formed from the primary profile by suppressing a long-wave component and serves as the basis for obtaining the surface profile parameters;

– waviness profile – is obtained by suppressing the long-wave and short-wave components, it is used to obtain the waviness parameters;

– geometrical parameters of the *P*, *R*, *W* groups – are calculated based on the primary profile, surface profile, and waviness profile, respectively.

In the design-engineering practice, a very limited list of parameters is used at the enterprises in the machine-building sector [1–3]. The parameters of the *R* and *W* groups are mainly used [4; 5], in particular, the *Ra*, *Rz* parameters, etc. At the same time, among the parameters little used in practice, *Ra* is one of the promising ones.

The analysis of publications on honing showed that when describing the requirements for surface roughness of parts, in most studies in the field of mechanical engineering, only the *Ra* parameter is given [6–8]. In some publications,

tp or *tp* and *Rz* are added to it [9]. In rare cases, *R*max and *Sm* are added to the above parameters [9]. In the literature, there are practically no parameters from new standards or specific parameters for describing the surface after honing from the less recent DIN standards of the 1980s. In recent years, the alternative methods for obtaining parameters have been actively developed, for example, new algorithms for correlating the parameters of a reflected beam from a microrelief [1]. These methods are being developed to detect all the same *Ra* type standard parameters [2].

Most of publications on honing associate the solution of the optimisation task with the application of theoretical and empirical models. The most common method is the Taguchi method [3]. The indicators of this method are used as an optimisation criterion [4]. An alternative method to achieve the same goal is the neural network method [5]. The authors also use the response surface analysis methods to determine the interrelation between the processing modes and technological parameters [6]. In these publications, only *Ra* was considered as a basic parameter.

The authors of [8] investigated the honing treatment using a magneto-rheological fluid. Interestingly, in this case, the meaning of the term "honing" no longer implies the use of a hone (tool for processing), but primarily the surface formed by this method. Similarly, there is a laser honing process that does not involve mechanical stock removal, but only energy impact. The authors state that the coincidence in the surface texture for the traditional method and the proposed one was 5.88 %. When describing the surface roughness, the authors give the *Ra* parameter. No other parameters were considered, despite the availability of a measuring device (Surftest SJ-400, Mitutoyo) sufficient for their evaluation.

In [9], the authors analyzed how to determine the surface texture using the widely known acoustic emission method. The authors propose two new parameters: *Sf* (calculated as the ratio of signals when applying high and low frequencies) and *Sh* (energy parameter). In this case, these parameters are correlated with the typical *Ra* parameters and the three-dimensional version of the *Ra* parameter – the *Sa* parameter. The work [9] confirms that interest in other methods for determining surface characteristics is high. However, this method will require the purchase of extra equipment for texture evaluation.

In [10], the authors give the reasoning of the theory of a new finishing process proposed as a functional replacement for honing. The surface was considered only from the point of view of the *Ra* parameter. In the paper [11], which describes the influence of changing a honing angle on the roughness and tribological properties, the *Ra* parameter and the *Rk* group (*Rpk, Rk, Rvk*) parameters are given. It is interesting, that the authors concluded that the *Rk* group parameters reflect the tribological characteristics more than the *Ra* parameter. The *Rk* group parameters were developed exactly for this. At the same time, in the conclusions, the authors carried out comparison according to the quantitative values not of *Rk*, but of *Ra* (the optimal value of the *Ra* parameter was 0.85).

The authors of the work [12], related to the evaluation of the tribological properties of a rough honed surface, by changing the contact pressure, evaluated the formed plateau-surface tribologically, dividing it qualitatively into two types: high and low. The basis for division was the authors' classification by the surface decomposed according to the frequencies with given (not variable) parameters over the *Rk* group.

The work [13] studied the influence of the hone radius on technological parameters (cutting force, surface integrity, etc.). The *Ra* parameter served as an estimate of the surface topography. In the conclusions, the smallest numerical value of the *Ra* parameter was considered as a criterion for the best surface.

The paper [14] examined multi-response optimisation to ensure the surface quality and performance. The authors do not directly name the parameters, they indicate the "maximum roughness" (probably *R*max) and "average roughness" (probably *Ra*). As a result, the authors built three models: for average and maximum roughness and for operation time. It was found that the grain size has the most influence on the average *Ra* value. As in the source [13], this conclusion is again obvious considering the mechanics of the process. At the same time, the authors position the presented three-factor optimisation model (two roughness parameters and operation time) as the most complete one.

The paper [15] presents an indirect neural network for modelling roughness during honing. The *Rk* group parameters are used. Using this model, the authors were able to predict the grain size, linear and tangential velocities, and pressure to obtain the specified values of the *Rk* group parameters. Reference [16] uses the results obtained from test honing machines for industrial application. In this paper, the authors supplement the *Rk* group parameters with the *Rz* parameter as necessary for industrial application.

In [17], the honing tool roughness was analyzed. Using two theories of roughness generation, the authors compared the calculated *Ra* parameter with the experimental one. An extensive analysis of the process kinematics (different angles, rotation speeds) was carried out; however, no other parameters except this one were considered.

New parameters are used to a small extent in the literature (Table 1). This is also typical for other studies of machining technologies that consider roughness [18].

Thus, there is a small quantity of parameters used in practice (no more than 6). The parameters available in international standards will allow determining the surface texture more accurately. In this work, the author proceeded with the development of the proposed earlier ideas on the development of a new method for determining the surface texture [19]. It is proposed to introduce into practice a little-used parameter – the profile physical coefficient. To assess the validity of the application of this approach, it is required to study the surface texture of the product according to the method proposed below for the parameter under consideration – the profile physical coefficient. Within this conception, the authors proposed to determine the most significant parameters and then find the range of optimal values for them, and not proceed from a specified limited list of parameters.

The proposed "profile physical coefficient" parameter can be denoted as $P_{mr(c)}$, $T_{mr(c)}$, and $W_{mr(c)}$ depending on the source of the initial data, and is calculated in general form by the following formula:

$$P_{mr(c)}, T_{mr(c)}, W_{mr(c)} = \frac{Ml(c)}{l_n}.$$

Table 1. *Texture parameters applied in the literature*
Таблица 1. *Применяемые в литературе параметры текстуры*

Specified texture parameters				Papers, where the structure parameters under consideration were applied
Ra	***R*max**	***Rk***	***Sa***	
+	–	–	–	[6]
+	–	–	–	[15]
+	–	–	+	[8]
+	–	–	–	[10]
+	–	+	–	[11]
–	–	+	–	[12]
+	–	–	–	[13]
+	+	–	–	[14]
+	+	+	+	[9]

The goal of the research is to develop a general approach to the application of the "profile physical coefficient" parameter and its testing.

METHODS

The technique is based on the assessment of the surface microprofile by the "profile physical coefficient" parameter.

First, the profile physical coefficient was determined at the sectional level. Next, it was expanded into a Fourier series for the two-dimensional and three-dimensional cases. As a result, the complexity of the presented parameter was shown.

Based on the geometrical representation of probability, the profile physical coefficient represents the probability of density of filling with a material in the selected section *c*.

The $P_{mr(c)}$, $T_{mr(c)}$, $W_{mr(c)}$ relative physical coefficient is determined at the sectional level of the $R\delta c$ profile relative to the starting point C_0:

$$P_{mr'}, T_{mr'}, W_{mr} = P_{mr'}, T_{mr'}, W_{mr}(C_1),$$

where $C_1 = C_0 - R_{\delta c}$ (or $P_{\delta c}$, or $W_{\delta c}$);
$C_0 = (CP_{mr0}, T_{mr0}, W_{mr0})$.

The difference between the profile relative physical coefficient $P_{mr(c)}$, $T_{mr(c)}$, $W_{mr(c)}$ and the widely known ones is that not filtered data are used (the parameters of the *R* – roughness group, such as *Ra, tp*), but the primary surface profile (hence the name of the group of parameters *P* – primary).

The profile of the surface relief obtained geometrically in two-dimensional space in the form of a profilogram can be represented analytically in the form of a trigonometric Fourier series:

$$Z(x) = \frac{a_0}{2} + \sum_{n=1}^{\infty} a_n \cos\frac{n\pi x}{l} + b_n \sin\frac{n\pi x}{l},$$

where

$$a_0 = \frac{1}{l}\int_{-l}^{l} Z(x)dx,$$

$$a_n = \frac{1}{l}\int_{-l}^{l} Z(x)\cos\frac{n\pi x}{l}dx,$$

$$b_n = \frac{1}{l}\int_{-l}^{l} Z(x)\sin\frac{n\pi x}{l}dx.$$

$$Z(x) = \begin{cases} Z_1(x), -l \le x \le -l + X_{S_1} \\ Z_2(x), -l + X_{S_1} \le x \le -l + X_{S_1} + X_{S_2} \\ \ldots \\ Z_\gamma(x), -l + \sum_{i=1}^{\gamma-1} X_{S_i} \le x \le -l + \sum_{i=1}^{\gamma}\left(-l + \sum_{i=1}^{\gamma} X_{S_i}\right) \\ Z_k(x), -l + \sum_{i=1}^{k-1} X_{S_i} \le x \le l \end{cases}.$$

In three-dimensional space, the surface topography is specified using a function of two variables $z = f(x,y)$, which can be expanded into a double trigonometric Fourier series in terms of a system of trigonometric functions. These functions represent a trigonometric system for two variables *x* and *y*, each of which is periodic with a period of 2π, both in *x* and *y*.

Each function of the system is orthogonal to any other in square $D(-\pi \le x \le \pi, -\pi \le y \le \pi)$. The specified property takes place in any other square of the form $a \le x \le a + 2\pi, -b \le y \le b + 2\pi$. The orthogonality property follows from the correlations

$$C_1 = C_0 - R_{\delta c}\iint_D 1\cdot\cos mx dxdy = \int_{-\pi}^{\pi} dy\int_{-\pi}^{\pi}\cos mx dx =$$
$$= \int_{-\pi}^{\pi}\left(\frac{1}{m}\left|\sin mx_{-\pi}^{\pi}\right.\right)dy = \frac{1}{m}\int_{-\pi}^{\pi}\left(\sin m\pi - \sin(-m\pi)\right)dy = 0 .$$

In a similar manner

$$\iint_D 1\cdot\sin mx dxdy = \int_{-\pi}^{\pi} dy\int_{-\pi}^{\pi}\sin mx dx =$$
$$= \int_{-\pi}^{\pi}\left(\frac{1}{m}\left|\cos mx_{-\pi}^{\pi}\right.\right)dy = \frac{1}{m}\int_{-\pi}^{\pi}\left(\cos m\pi - \cos(-m\pi)dy\right) = ,$$
$$= -\frac{1}{m}\int_{-\pi}^{\pi}\left(\cos m\pi - \cos m\pi\right)dy = 0$$

as the cos$n\pi$ function is even, then $\cos(-n\pi) = \cos(n\pi)$. As a consequence,

$$\int_D (\cos mx\cos ny)(\cos rx\cos px)\,dxdy =$$
$$= \int_{-\pi}^{\pi}\cos mx\cos rx\left(\int_{-\pi}^{\pi}\cos nx\cos pydy\right)dx =$$
$$= \int_{-\pi}^{\pi}\cos mx\cos rxdx\int_{-\pi}^{\pi}\cos nx\cos pydy = ,$$
$$= \frac{1}{4}\int_{-\pi}^{\pi}\left[\cos(m+r)x + \cos(m-r)x\right]\times$$
$$\times\int_{-\pi}^{\pi}\left[\cos(n+p)x + \cos(n-p)y\right]dy = 0$$

where r and p are integers, at $m \neq r$, $n \neq p$.

It was proved above that the integral in the symmetric region of an even function vanishes when $m = r$ и $n = p$, then the original integral takes the form

$$\int_{-\pi}^{\pi}\cos^2 mxdx\cdot\int_{-\pi}^{\pi}\cos^2 nydy =$$
$$= \frac{1}{2}\int_{-\pi}^{\pi}(1+\cos 2mx)dx\cdot\frac{1}{2}\int_{-\pi}^{\pi}(1+\cos 2ny)dy =$$
$$= \frac{1}{2}\left[2\pi + \frac{1}{2}\left|\sin 2mx_{-\pi}^{\pi}\right.\right]\cdot\frac{1}{2}\left[2\pi + \frac{1}{2}\left|\sin 2ny_{-\pi}^{\pi}\right.\right] =$$
$$= \frac{1}{4}\cdot 4\pi^2 = \pi^2$$

Here, $\sin 2mx_{-\pi}^{\pi} = \sin 2m\pi - \sin(-2m\pi) = 0$ since $\sin m\pi = 0$.

The orthogonality of any pair of different functions of the original trigonometric system is proved similarly.

We define the norms of the elements of the presented trigonometric system:

$$\|1\| = \sqrt{\iint_D dxdy} = \sqrt{4\pi^2} = 2\pi ,$$

$$\|\cos mx\| = \|\sin mx\| = \|\cos ny\| = \|\sin ny\| = \sqrt{2}\pi ,$$

$$\|\cos mx\| = \sqrt{\iint_D \cos^2 mdxdy} = \sqrt{\int_{-\pi}^{\pi} dy\int_{-\pi}^{\pi}\cos^2 mxdx} =$$
$$= \sqrt{\int_{-\pi}^{\pi}\frac{1}{2}(1+)\left|\cos m_{-\pi}^{\pi}dy\right.} = \sqrt{\frac{1}{2}\cdot 2\pi\cdot 2\pi} = \sqrt{2}\pi ,$$

$$\|\cos mx\cdot\cos ny\| = \|\sin mx\cdot\cos ny\| =$$
$$= \|\cos my\cdot\sin ny\| = \|\sin nx\cdot\sin ny\| = \pi ,$$

$$\|\cos mx\cdot\cos ny\| = \sqrt{\int_D \cos^2 mx\cdot\cos^2 ny\cdot dxdy} =$$
$$= \sqrt{\int_{-\pi}^{\pi}\cos^2 mxdx\int_{-\pi}^{\pi}\cos^2 nydy} = \sqrt{\frac{1}{4}\cdot\frac{\pi^2}{4}} = \pi .$$

As in the case of a one-variable function $z = f(x)$, the Fourier coefficients for a two-variable function $z = f(x;y)$ defined in the domain D are found from the correlations [3]:

$$A_{00} = \frac{\iint_D f(x;y)dxdy}{\|1\|^2} = \frac{1}{4\pi^2}\iint_D f(x;y)dxdy ,$$

$$A_{m0} = \frac{\iint_D [f(x;y)\cos mx]dxdy}{\|\cos mx\|^2} =$$
$$= \frac{1}{2\pi^2}\iint_D [f(x;y)\cos mx]dxdy, m = 1, 2, ..., \infty ,$$

$$A_{0n} = \frac{\iint_D [f(x;y)\cos ny]dxdy}{\|\cos ny\|^2} =$$
$$= \frac{1}{2\pi^2}\iint_D [f(x;y)\cos ny]dxdy, n = 1, 2, ..., \infty ,$$

$$B_{m0} = \frac{\iint_D [f(x;y)\sin mx]dxdy}{\|\sin mx\|^2} =$$
$$= \frac{1}{2\pi^2}\iint_D [f(x;y)\sin mx]dxdy, m = 1, 2, ..., \infty ,$$

$$B_{0n} = \frac{\iint_D [f(x;y)\sin ny]dxdy}{\|\sin ny\|^2} =$$
$$= \frac{1}{2\pi^2}\iint_D [f(x;y)\sin ny]dxdy, n = 1, 2, ..., \infty .$$

If m and n both possess the values $m = 1, 2, ..., \infty$, $n = 1, 2, ..., \infty$, then:

$$a_{m.n} = \frac{1}{\pi^2}\iint_D [f(x;y)\cos mx\cdot\cos ny]dxdy ,$$

$$b_{m.n} = \frac{1}{\pi^2}\iint_D [f(x;y)\sin mx\cdot\cos ny]dxdy ,$$

$$c_{m.n} = \frac{1}{\pi^2}\iint_D [f(x;y)\cos mx \cdot \sin ny]dxdy ,$$

$$d_{m.n} = \frac{1}{\pi^2}\iint_D [f(x;y)\sin mx \cdot \sin ny]dxdy .$$

In practical problems, instead of A_{00}, it is advisable to denote $\frac{a_{00}}{4}$, where a_{00} is found from am,n at $m = 0$ and $n = 0$. Similarly, instead of $Am,0$, $A0,n$, $Bm,0$, $B0,n$, we write $\frac{a_{m,0}}{2}, \frac{a_{0,n}}{2}, \frac{b_{m,0}}{2}, \frac{b_{0,n}}{2}$, which are calculated from the expressions am,n , bm,n, cm,n, dm,n when given $m = 1, 2, \ldots, \infty$, $n = 0$ or $n = 1, 2, \ldots, \infty$, $m = 0$. As a result, the double trigonometric series is written as:

$$z = f(x;y) = \sum_{m=0}^{\infty}\sum_{n=0}^{\infty}\lambda_{m.n}\begin{bmatrix} a_{m.n}\cos mx \cdot \cos ny + \\ + b_{m.n}\sin mx \cdot \cos ny + \\ + c_{m.n}\cos mx \cdot \sin ny + \\ + d_{m.n}\sin mx \cdot \sin ny \end{bmatrix},$$

here

$$\lambda = \begin{cases} \frac{1}{4}, \text{ при } m = n = 0 \\ 1, \text{ при } m > 0, n > 0 \\ \frac{1}{2}, \text{ при } m > 0, n = 0 \text{ или } m = 0, n > 0 \end{cases},$$

in this case m and n are positive integers.

In the case when the domain D_Ξ is represented by a rectangle that meets the conditions D_Ξ ($-lx < x < lx$, $-ly < y < ly$) (Fig. 1), the double Fourier series takes the form:

$$z = f(x;y) = \sum_{m=0}^{\infty}\sum_{n=0}^{\infty}\lambda_{m.n}\begin{bmatrix} a_{m.n}\cos m\frac{\pi}{l_x}x \cdot \cos n\frac{\pi}{l_y}y + \\ + b_{m.n}\sin \frac{\pi}{l_x}mx \cdot \cos n\frac{\pi}{l_y}y + \\ + c_{m.n}\cos m\frac{\pi}{l_x}x \cdot \sin n\frac{\pi}{l_y}y + \\ + d_{m.n}\sin m\frac{\pi}{l_x}x \cdot \sin n\frac{\pi}{l_y}y \end{bmatrix}.$$

The λ_{mn} parameter is found according to the correlations written above, and the $am.n$, $bm.n$, $cm.n$, $dm.n$ coefficients are calculated using the formulas:

$$a_{m.n} = \frac{1}{l_x l_y}\iint_{D_\Xi}\left[f(x;y)\cos m\frac{\pi}{l_x}x \cdot \cos n\frac{\pi}{l_y}y \right]dxdy ,$$

$$b_{m.n} = \frac{1}{l_x l_y}\iint_{D}\left[f(x;y)\sin m\frac{\pi}{l_x}x \cdot \cos n\frac{\pi}{l_y}y \right]dxdy ,$$

$$c_{m.n} = \frac{1}{l_x l_y}\iint_{D}\left[f(x;y)\cos m\frac{\pi}{l_x}x \cdot \sin n\frac{\pi}{l_y}y \right]dxdy ,$$

$$d_{m.n} = \frac{1}{l_x l_y}\iint_{D}\left[f(x;y)\sin m\frac{\pi}{l_x}x \cdot \sin n\frac{\pi}{l_y}y \right]dxdy .$$

In the special case when $lx = ly = \pi$, the previous expressions for the square domain D_Ξ are obtained from the written expressions. In the case when the function $z(x; y)$ is specified as piecewise smooth in the domains Di, $i = 1, 2, \ldots, n$:

$$z(x;y) = \begin{cases} f_1(x,y), \text{ при } (x;y) \subset D_1 \\ f_2(x,y), \text{ при } (x;y) \subset D_2 \\ \ldots \\ f_k(x,y), \text{ при } (x;y) \subset D_k \end{cases},$$

the double trigonometric series will be analogous to the Fourier series of similar one-variable functions.

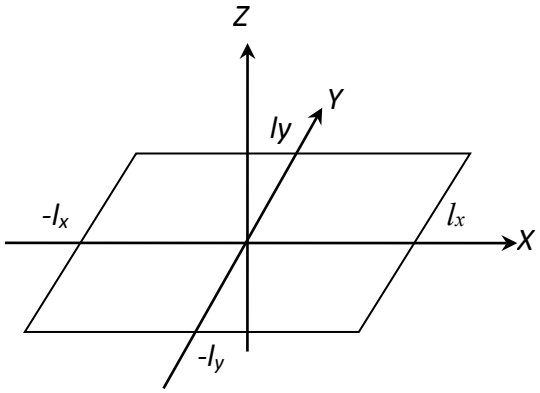

Fig. 1. *Rectangular area D_Ξ in the XOY plane*
Рис. 1. *Прямоугольная область D_Ξ в плоскости XOY*

Surface texture characteristics are predominantly geometric. However, when processing and operating the machine parts and mechanisms, physical indicators are used, such as material removal in various technologies, wear, friction, elasticity, and the rough layer plastic deformation caused by the presence of the material in it.

The complex parameter for evaluating these phenomena is the analyzed profile physical coefficient regulated by the international standard and representing the probability of density of filling with the material in the z section, i.e. $P(VMc)$, according to the geometric concept of probability.

The probability of material content in a rough layer of width c is determined by the formula

$$P(V_{Mc}) = \int_0^c P_{mr((z))}dz .$$

RESULTS

It is possible to test the considered method on the profillogram of the surface of a honed part.

If a profillogram is obtained for a rough layer, where $c = zk$ measured from the OX axis, then the profile physical coefficient from geometric constructions is determined by the formula

$$P_{mr}(z_k) = \frac{\sum_{i=1}^{k_c} Mli}{\sum_{j=1}^{k_c} Mlj},$$

where kc – is the number of sections of the material in the c section.

Specifically for the present case, Rz = 74 mm is divided into k = 10 parts, ln = 155 mm. The results of measurements and calculations are summarized in Table 2 and presented graphically in Fig. 2. Probability of filling the rough layer with the material

$$P(V_m) = \frac{S_m}{R_k \cdot l_n},$$

where Sm – is the area of the figure enclosed by a curve Ml_{Zk}.

Let us find the value of Sm:

$$S_m = \frac{R_Z}{6m}\left(\frac{Ml_0}{2} + 2\sum_{i=1}^{2m-2} Ml_{2i} + 4\sum_{i=1}^{2m-1} Ml_{2i-1}\right), m = 51,$$

$$S_m = \frac{R_Z}{6 \cdot 5}\left[\begin{matrix}748 + 2(151{,}2 + 128{,}1 + 71{,}2 + 34{,}8) + \\ + 4(153{,}6 + 141{,}8 + 83{,}6 + 51{,}9 + 5{,}5)\end{matrix}\right] =$$

$$= R_Z \cdot 86{,}23$$

$$P(V_m) = \frac{R_Z \cdot 86{,}23}{l_n} = \frac{1}{l_n} 86{,}23 = 0{,}5563.$$

The calculation shows that for a rough layer with a given profillogram, the probability of filling it with the material is equal to 0.5563, i.e., the given rough layer contains 55.63 % of the material. The porosity coefficient λ is the characteristic of voids in the specified layer:

$$\lambda = \frac{S_{сл} - S_h}{S_{сл}} = 1 - \frac{S_m}{S_{сл}} 1 - P(V_m),$$

where $S_{сл}$ – is the total area of a rough layer on the length ln, $S_{сл} = Rz \cdot ln$.

Thus, λ = 1 $-P(V_m)$, oil-absorption is 44.37 %.

Table 2. *Calculation of the probability of the density of filling the rough layer with the material along the zi sections*
Таблица 2. *Расчет вероятности плотности заполнения материалом шероховатого слоя по сечениям zi*

z_i	z_0 **0**	z_1 **7.4**	z_2 **14.8**	z_3 **22.2**	z_4 **29.6**	z_5 **37**	z_6 **44.4**	z_7 **51.8**	z_8 **59.2**	z_9 **66.6**	z_{10} **74**
S_{zi}	155	153.6	151.2	141.1	128.1	83.6	71.2	51.9	34.2	5.5	0
$P(S_{zi})$	1	0.991	0.975	0.910	0.826	0.539	0.459	0.335	0.221	0.035	0

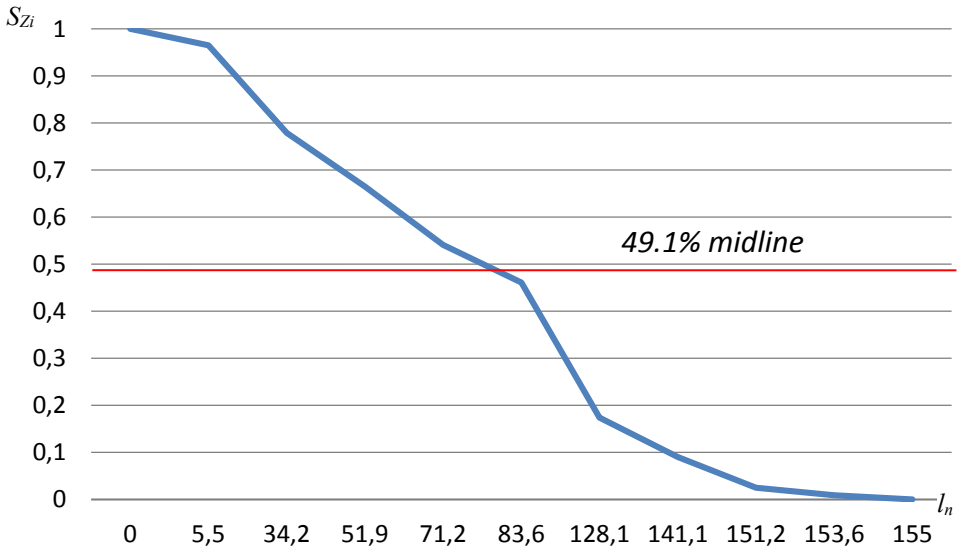

Fig. 2. *The curve of the probability of filling the rough layer with the material along the sections corresponding to the actual profillogram*
Рис. 2. *Кривая вероятности заполнения материалом шероховатого слоя по сечениям, соответствующая реальной профилограмме*

DISCUSSION

Currently, the surface texture parameters used in practice, presented in publications and in production, are insufficient. The use of complex parameters reflecting the operational characteristics of products is required. As part of the work performed, the authors justified the use of the "profile physical coefficient" parameter for estimating the surface texture using a new technique. The use of the profile physical coefficient allows meeting the increasing requirements for the working conditions of the surfaces of parts, especially those operating under friction conditions. Knowledge of the properties of the proposed models will allow recommending the technologies and methods for processing surfaces of interacting parts of machines and mechanisms.

The parameter was tested for a honed surface, and convergence was shown when analyzing the filling of a rough layer with a material along sections, which corresponds to the actual profillogram.

According to the developed technique, the Fourier series expansion of the micro-roughness model profile function given in the interval $(-l; l)$ allows building the entire range of models on a line of selective length according to which the profillogram is reproduced. It is important that in the overall assessment of the working surface microdimensions, it is possible to take into account deviations from a given geometric shape of the part, both regular and random.

A probabilistic assessment of filling the layer with the material from the theoretical reference line or surface to the theoretical equidistant line of the real profile is necessary when developing software for technological equipment operating in automatic control of cutting, grinding, honing, and plastic deformation in the process of forming the texture of the working surface of finished parts.

In future, the developed method for the computational-graphical study of a surface texture can be applied to analyze and evaluate the texture of the surfaces processed by various technologies, including the evaluation of the surface after post-processing of parts obtained additively.

The effect of applying the proposed method for estimating surface texture can be increased when combining it with new processing methods and techniques that contribute to the formation of a given surface texture.

CONCLUSIONS

The author justified the application of the "profile physical coefficient" parameter to set the requirements for the micro-geometry of the working surfaces of the parts.

The analysis of the obtained quantitative parameters found based on profillograms proved that the assessment of the material consumption of a rough layer most completely and comprehensively, compared to the well-known and widely used *Ra* parameter, characterises the geometry of waviness, its shape, flatness, pointedness, relief, performance, wear resistance, and oil absorption of voids and, accordingly, allows innovating the assessment of mixed friction of real surfaces.

REFERENCES

1. Abramov A., Bobrovskij N.M., Nosov N.V., Tabakov V., Galyalieva K. Quasi-optimal correlation algorithm for measuring the parameters of surface microrelief. *Key Engineering Materials*, 2019, vol. 822, pp. 725–730. DOI: 10.4028/www.scientific.net/KEM.822.725.
2. Abramov A., Bobrovskij S.M., Nosov N.V., Tabakov V., Lopatina F. Method for determining texture parameters of processed precision surfaces by correlation. *Key Engineering Materials*, 2019, vol. 822, pp. 731–736. DOI: 10.4028/www.scientific.net/KEM.822.731.
3. Singh R.V., Raghav A.K. Experimental study and modelling of the effect of process parameters on surface roughness during honing process. *Journal of the Institution of Engineers (India). Part PR: Production Engineering Division*, 2010, vol. 90, pp. 3–7.
4. Neagu C., Dumitrescu A. Neural networks modelling of process parameters in honing of thermal engines' cylinders. *Metalurgia International*, 2008, vol. 13, no. 5, pp. 66–78.
5. Feng C.-X.J., Yu Z.-G.S., Kingi U., Pervaiz B.M. Threefold vs. fivefold cross validation in one-hidden-layer and two-hidden-layer predictive neural network modeling of machining surface roughness data. *Journal of Manufacturing Systems*, 2005, vol. 24, no. 2, pp. 93–107. DOI: 10.1016/S0278-6125(05)80010-X.
6. Silva S.P., Brandao L.C., Pimenta P.R.F. Evaluation of quality of steering systems using the honing process and surface response methodology. *Advanced Materials Research*, 2011, vol. 223, pp. 821–825. DOI: 10.4028/www.scientific.net/AMR.223.821.
7. Tripathi B.N., Singh N.K., Vates U.K. Surface roughness influencing process parameters & modeling techniques for four stroke motor bike cylinder liners during honing: Review. *International Journal of Mechanical and Mechatronics Engineering*, 2015, vol. 15, no. 1, pp. 106–112.
8. Paswan S.K., Bedi T.S., Singh A.K. Modeling and simulation of surface roughness in magnetorheological fluid based honing process. *Wear*, 2017, vol. 376-377, pp. 1207–1221. DOI: 10.1016/j.wear.2016.11.025.
9. Buj-Corral I., Álvarez-Flórez J., Domínguez-Fernández A. Acoustic emission analysis for the detection of appropriate cutting operations in honing processes. *Mechanical Systems and Signal Processing*, 2018, vol. 99, pp. 873–885. DOI: 10.1016/j.ymssp.2017.06.039.
10. Span J., Koshy P., Klocke F., Müller S., Coelho R. Dynamic jamming in dense suspensions: Surface finishing and edge honing applications. *CIRP Annals*, 2017, vol. 66, no. 1, pp. 321–324. DOI: 10.1016/j.cirp.2017.04.082.
11. Ma S., Liu Y., Wang Z., Wang Zh., Huang R., Xu J. The Effect of Honing Angle and Roughness Height on the Tribological Performance of CuNiCr Iron Liner. *Metals*, 2019, vol. 9, no. 5, article number 487. DOI: 10.3390/met9050487.
12. Hu Y., Meng X., Xie Y., Fan J. Mutual influence of plateau roughness and groove texture of honed surface on frictional performance of piston ring-liner system. *Proceedings of the Institution of Mechanical Engineers, Part J: Journal of Engineering Tribology*, 2017, vol. 231, no. 7, pp. 838–859. DOI: 10.1177/1350650116682161.
13. Li B., Zhang S., Yan Z., Jiang D. Influence of edge hone radius on cutting forces, surface integrity, and surface oxidation in hard milling of AISI H13 steel. *Inter-*

national Journal of Advanced Manufacturing Technology, 2018, vol. 95, pp. 1153–1164. DOI: 10.1007/s00170-017-1292-z.
14. Nguyen T.-T., Vu T.-C., Duong Q.-D. Multi-responses optimization of finishing honing process for surface quality and production rate. *Journal of the Brazilian Society of Mechanical Sciences and Engineering*, 2020, vol. 42, article number 604. DOI: 10.1007/s40430-020-02690-y.
15. Arantes L.J., Fernandes K.A., Schramm C.R., Leal J.E.S., Piratelli-Filho A., Franco S.D., Arencibia R.V. The roughness characterization in cylinders obtained by conventional and flexible honing processes. *The International Journal of Advanced Manufacturing Technology*, 2017, vol. 93, pp. 635–649. DOI: 10.1007/s00170-017-0544-2.
16. Buj-Corral I., Rodero-De-Lamo L., Marco-Almagro L. Use of results from honing test machines to determine roughness in industrial honing machines. *Journal of Manufacturing Processes*, 2017, vol. 28, pp. 60–69. DOI: 10.1016/j.jmapro.2017.05.016.
17. Yuan B., Han J., Wang D., Zhu Y., Xia L. Modeling and analysis of tooth surface roughness for internal gearing power honing gear. *Journal of the Brazilian Society of Mechanical Sciences and Engineering*, 2017, vol. 39, pp. 3607–3620. DOI: 10.1007/s40430-017-0791-z.
18. Kuznetsov V.P., Voropaev V.V., Skorobogatov A.S. Finishing and hardening of a flat surface ring area of a workpiece by rotary burnishing. *Key Engineering Materials*, 2017, vol. 743, pp. 245–247. DOI: 10.4028/www.scientific.net/KEM.743.245.
19. Bobrovskii I.N. How to Select the most Relevant Roughness Parameters of a Surface: Methodology Research Strategy. *IOP Conference Series: Materials Science and Engineering*, 2018, vol. 302, article number 012066. DOI: 10.1088/1757-899X/302/1/012066.

СПИСОК ЛИТЕРАТУРЫ

1. Abramov A., Bobrovskij N.M., Nosov N.V., Tabakov V., Galyalieva K. Quasi-optimal correlation algorithm for measuring the parameters of surface microrelief // Key Engineering Materials. 2019. Vol. 822. P. 725–730. DOI: 10.4028/www.scientific.net/KEM.822.725.
2. Abramov A., Bobrovskij S.M., Nosov N.V., Tabakov V., Lopatina F. Method for determining texture parameters of processed precision surfaces by correlation // Key Engineering Materials. 2019. Vol. 822. P. 731–736. DOI: 10.4028/www.scientific.net/KEM.822.731.
3. Singh R.V., Raghav A.K. Experimental study and modelling of the effect of process parameters on surface roughness during honing process // Journal of the Institution of Engineers (India). Part PR: Production Engineering Division. 2010. Vol. 90. P. 3–7.
4. Neagu C., Dumitrescu A. Neural networks modelling of process parameters in honing of thermal engines’ cylinders // Metalurgia International. 2008. Vol. 13. № 5. P. 66–78.
5. Feng C.-X.J., Yu Z.-G.S., Kingi U., Pervaiz B.M. Threefold vs. fivefold cross validation in one-hidden-layer and two-hidden-layer predictive neural network modeling of machining surface roughness data // Journal of Manufacturing Systems. 2005. Vol. 24. № 2. P. 93–107. DOI: 10.1016/S0278-6125(05)80010-X.
6. Silva S.P., Brandao L.C., Pimenta P.R.F. Evaluation of quality of steering systems using the honing process and surface response methodology // Advanced Materials Research. 2011. Vol. 223. P. 821–825. DOI: 10.4028/www.scientific.net/AMR.223.821.
7. Tripathi B.N., Singh N.K., Vates U.K. Surface roughness influencing process parameters & modeling techniques for four stroke motor bike cylinder liners during honing: Review // International Journal of Mechanical and Mechatronics Engineering. 2015. Vol. 15. № 1. P. 106–112.
8. Paswan S.K., Bedi T.S., Singh A.K. Modeling and simulation of surface roughness in magnetorheological fluid based honing process // Wear. 2017. Vol. 376-377. P. 1207–1221. DOI: 10.1016/j.wear.2016.11.025.
9. Buj-Corral I., Álvarez-Flórez J., Domínguez-Fernández A. Acoustic emission analysis for the detection of appropriate cutting operations in honing processes // Mechanical Systems and Signal Processing. 2018. Vol. 99. P. 873–885. DOI: 10.1016/j.ymssp.2017.06.039.
10. Span J., Koshy P., Klocke F., Müller S., Coelho R. Dynamic jamming in dense suspensions: Surface finishing and edge honing applications // CIRP Annals. 2017. Vol. 66. № 1. P. 321–324. DOI: 10.1016/j.cirp.2017.04.082.
11. Ma S., Liu Y., Wang Z., Wang Zh., Huang R., Xu J. The Effect of Honing Angle and Roughness Height on the Tribological Performance of CuNiCr Iron Liner // Metals. 2019. Vol. 9. № 5. Article number 487. DOI: 10.3390/met9050487.
12. Hu Y., Meng X., Xie Y., Fan J. Mutual influence of plateau roughness and groove texture of honed surface on frictional performance of piston ring-liner system // Proceedings of the Institution of Mechanical Engineers, Part J: Journal of Engineering Tribology. 2017. Vol. 231. № 7. P. 838–859. DOI: 10.1177/1350650116682161.
13. Li B., Zhang S., Yan Z., Jiang D. Influence of edge hone radius on cutting forces, surface integrity, and surface oxidation in hard milling of AISI H13 steel // International Journal of Advanced Manufacturing Technology. 2018. Vol. 95. P. 1153–1164. DOI: 10.1007/s00170-017-1292-z.
14. Nguyen T.-T., Vu T.-C., Duong Q.-D. Multi-responses optimization of finishing honing process for surface quality and production rate // Journal of the Brazilian Society of Mechanical Sciences and Engineering. 2020. Vol. 42. Article number 604. DOI: 10.1007/s40430-020-02690-y.
15. Arantes L.J., Fernandes K.A., Schramm C.R., Leal J.E.S., Piratelli-Filho A., Franco S.D., Arencibia R.V. The roughness characterization in cylinders obtained by conventional and flexible honing processes // The International Journal of Advanced Manufacturing Technology. 2017. Vol. 93. P. 635–649. DOI: 10.1007/s00170-017-0544-2.
16. Buj-Corral I., Rodero-De-Lamo L., Marco-Almagro L. Use of results from honing test machines to determine roughness in industrial honing machines // Journal of Manufacturing Processes. 2017. Vol. 28. P. 60–69. DOI: 10.1016/j.jmapro.2017.05.016.
17. Yuan B., Han J., Wang D., Zhu Y., Xia L. Modeling and analysis of tooth surface roughness for internal

gearing power honing gear // Journal of the Brazilian Society of Mechanical Sciences and Engineering. 2017. Vol. 39. P. 3607–3620. DOI: 10.1007/s40430-017-0791-z.
18. Kuznetsov V.P., Voropaev V.V., Skorobogatov A.S. Finishing and hardening of a flat surface ring area of a workpiece by rotary burnishing // Key Engineering Materials. 2017. Vol. 743. P. 245–247. DOI: 10.4028/www.scientific.net/KEM.743.245.
19. Bobrovskii I.N. How to Select the most Relevant Roughness Parameters of a Surface: Methodology Research Strategy // IOP Conference Series: Materials Science and Engineering. 2018. Vol. 302. Article number 012066. DOI: 10.1088/1757-899X/302/1/012066.

Физический коэффициент профиля и его применение для моделирования текстуры механически обработанной поверхности

Бобровский Игорь Николаевич, доктор технических наук, научный сотрудник
Тольяттинский государственный университет, Тольятти (Россия)

E-mail: bobri@yandex.ru ORCID: https://orcid.org/0000-0002-9513-7936

Поступила в редакцию 28.07.2022 *Принята к публикации 14.04.2023*

Аннотация: Современные тенденции развития машиностроения задают всё более жесткие требования к эксплуатационным характеристикам готовой продукции. Основными параметрами, характеризующими качество изделия в целом, являются физико-механические и геометрические показатели рабочих поверхностей составных деталей. Поверхность, полученная в результате механической обработки, в отечественной практике в основном характеризуется весьма ограниченным числом параметров (не более 6), таких как средняя высота микронеровностей, высоты микронеровностей по 10 точкам и др. Однако их применение недостаточно для производства конкурентоспособной продукции в современных условиях. Например, международные стандарты ISO/ASME/DIN включают гораздо более широкий набор параметров, необходимых для точного описания эксплуатационных свойств поверхности. В статье проанализированы подходы к формированию требований к микрогеометрии рабочих поверхностей деталей, используемых в современном машиностроении. На основе проведенного анализа предложен и математически обоснован общий подход к моделированию характеристик текстуры поверхности, который позволяет адекватно описывать поверхность с использованием нового параметра – физического коэффициента профиля, поскольку прямое сравнение технологий, разработанных в России, с иностранными аналогами с опорой на действующие стандарты практически невозможно. Сначала был определен физический коэффициент профиля на секционном уровне. Далее было выполнено его разложение на ряд Фурье для двухмерного и трехмерного случаев. Приведен анализ применимости нового параметра на примере изделия, полученного с помощью хонингования. Сделан вывод о целесообразности применения данного параметра и необходимости разработки комплексной методики оценки поверхности после механической обработки на его основе.

Ключевые слова: технология машиностроения; механическая обработка; поверхность; физический коэффициент профиля; шероховатый слой; текстура поверхности.

Благодарности: Исследование выполнено за счет гранта Российского научного фонда № 20-79-00233, https://rscf.ru/project/20-79-00233/.

Для цитирования: Бобровский И.Н. Физический коэффициент профиля и его применение для моделирования текстуры механически обработанной поверхности // Frontier Materials & Technologies. 2023. № 3. С. 9–17. DOI: 10.18323/2782-4039-2023-3-65-1.